Stability of the Chlorinated Derivatives of the DNA/RNA Nucleobases, Purine and Pyrimidine toward Radical Formation via Homolytic C–Cl Bond Dissociation

Laura Kaliyeva,[a] Shingis Zhumagali,[b] Nuriya Akhmetova,[b] Amir Karton[c], Robert J. O'Reilly,[b,*]

[a]Department of Chemical Engineering, School of Engineering, Nazarbayev University, Astana, 010000, Republic of Kazakhstan. [b]Department of Chemistry, School of Science and Technology, Nazarbayev University, Astana, 010000, Republic of Kazakhstan. [c]School of Chemistry and Biochemistry, The University of Western Australia, Perth, WA 6009, Australia

Abstract

The chlorinated derivatives of nucleobases (and nucleosides), as well as those of purine, have well-established anticancer activity, and in some cases, are also shown to be involved in the link between chronic inflammatory conditions and the development of cancer. In this investigation, the stability of all of the isomeric forms of the chlorinated nucleobases, purine and pyrimidine are investigated from the perspective of their homolytic C–Cl bond dissociation energies (BDEs). The products of these reactions, namely chlorine atom and the corresponding carbon-centered radicals, may be of importance in terms of potentiating biological damage. Initially, the performance of a wide range of contemporary theoretical procedures were evaluated for their ability to afford accurate C–Cl BDEs, using a recently reported set of 28 highly-accurate C–Cl BDEs obtained by means of W1w theory. Subsequent to this analysis, the G3X(MP2)-RAD procedure (which achieves a mean absolute deviation of merely 1.3 kJ mol^{-1}, with a maximum deviation of 5.0 kJ mol^{-1}) was employed to obtain accurate gas-phase homolytic C–Cl bond dissociation energies for a wide range of chlorinated isomers of the DNA/RNA nucleobases, purine and pyrimidine.

Corresponding author (R. J. O'Reilly): robert.o'reilly@nu.edu.kz

Introduction

A number of the chlorinated derivatives of the DNA/RNA nucleobases (or nucleosides), as well as those of purine (for which adenine and guanine are derivatives), are known to exhibit anti-cancer activity. For example, 2-chloro-2'-deoxyadenosine (also known as Cladribine), is currently used for the treatment of conditions such as hairy cell leukemia,[1,2] and is also being investigated for treating multiple sclerosis.[3,4] 2-Chloroadenine, the major catabolite of Cladribine, has been shown to induce apoptosis in EHEB cells,[5] and is being investigated for use in patients with leukemia.[6] 6-chloropurine has been shown to retard the growth of Sarcoma 180 in mice,[7] and has also been shown to potentiate tumor inhibition in mice bearing the Ehrlich carcinoma when used in conjunction with azaserine.[8] The thymine derivative, 6-chlorothymine has also been shown to inhibit the growth of solid Ehrlich carcinomas.[9]

Certain chlorinated nucleobase derivatives have also been implicated in the development of cancers arising as a result of chronic inflammatory conditions. For example, the reaction of cytosine with hypochlorous acid (which is produced in vivo during the inflammatory process by way of the oxidation of chloride ion by H_2O_2 and catalyzed by the enzyme myeloperoxidase) has been shown to afford 5-chlorocytosine, which appears to be intrinsically mutagenic, inducing C→T transitions.[10] In addition, it has been shown that incorporation of 5-chlorocytosine into mammalian DNA results in heritable gene silencing and altered cytosine methylation patterns.[11] The pyrimidine derivative 5-Chlorouridine has demonstrated activity as a mutagen, clastogen and is an effective inducer of sister-chromatid exchange.[12,13] Hypochlorous acid-induced chlorination of guanine, affording 8-chloro-2'-deoxyguanosine has been also been reported previously.[14]

Given the immense interest in the chlorinated nucleobase and purine derivatives for use as pharmaceuticals for the treatment of conditions such as cancer, or because of their link between chronic inflammatory conditions and the development of cancers, understanding the factors that affect the structure and stability of such species is of great significance. From the perspective of structure, the relative energies of the various tautomeric forms of the chlorinated nucleobases have been examined in the cases of, for example, 5-chlorocytosine,[15,16] 5- and 6-chlorouracil,[17] and 2-chloroadenine.[18,19] On the other hand, accurate data concerning the energies necessary to induce homolytic cleavage of the C–Cl bonds of the chlorinated derivatives of the nucleobases, as well as those of purine and pyrimidine (i.e., the homolytic bond dissociation

energies), processes that afford chlorine atom and the corresponding carbon-centered radicals, have not been reported. It should be noted however that some data pertaining to the dissociation of the radical anions, not the closed-shell neutral forms, of species such as 5-chlorouracil[20] and 2-chloroadenine[21] (obtained using relatively low-level quantum chemical calculations) can be found in the literature. Consequently, a void still exists in our understanding of the stability of the neutral closed-shell chlorinated derivatives of the nucleobases, purine and pyrimidine, toward the formation of potentially damaging free radicals under non-reducing conditions.

With the ever increasing computational power of supercomputers and the development of computationally economical composite ab initio methods,[22,23,24] it is possible to obtain highly accurate thermochemical data for biologically relevant molecules such as amino acids and DNA bases (see refs. 25,26,27,28,29,30,31,32 for some recent studies). In the context of the present study it is important to obtain accurate C–Cl BDEs for chlorinated DNA bases in order to establish which carbon-centered radicals are likely to be formed with the greatest ease under certain biochemical conditions. However, given the necessarily approximate nature of composite ab initio methods, and density functional theory (DFT) methods, it is not a priori clear which methods will perform reliably for the computation of homolytic C–Cl BDEs. As a consequence, before proceeding to report homolytic C–Cl BDEs for the chlorinated derivatives of the nucleobases, purine and pyrimidine, it is initially of interest to identify suitable lower-cost theoretical procedures that may be employed in order to obtain accurate BDEs for these species. However, given the approximate nature of such methods, it is not *a priori* clear which methods will perform reliably for a given task. As a consequence, before proceeding to report homolytic C–Cl BDEs for the chlorinated derivatives of the nucleobases, purine and pyrimidine, it is initially of interest to identify suitable lower-cost theoretical procedures that may be employed in order to obtain accurate BDEs for these species.

Consequently, in the present investigation, initial attention is given to evaluating the performance of a wide range of quantum chemical methods for the computation of such quantities. To facilitate this analysis, the methods are evaluated against the recently reported dataset of 28 homolytic C–Cl BDEs (known as the CCl28 dataset)[33] obtained using the benchmark-quality W1w thermochemical protocol.[34] Having identified, as a result of this initial investigation, that the G3X(MP2)-RAD protocol offers an attractive cost:performance ratio, this method has been employed in order to obtain BDEs associated with the dissociation of the C–Cl

bonds of the chlorinated derivatives of the nucleobases (namely 2-chloroadenine, 5-chlorocytosine, 5-chlorouracil, 6-chlorocytosine, 6-chlorothymine, 6-chlorouracil, 8-chloroadenine and 8-chloroguanine), as well as all the possible chlorinated isomers of pyrimidine (namely the 2-, 4- and 5-chloro derivatives) and purine (namely the 2-, 6-, and 8-chloro derivatives). Consequently, this study offers valuable insights concerning the stability of these biologically-important species toward the formation of damaging radical species.

Computational Details

Using a set of 28 accurate homolytic C–Cl BDEs,[33] obtained using the high-level W1w thermochemical protocol[34] as reference values, the performance of a wide range of contemporary quantum chemical methods have been assessed for the ability to accurately compute gas-phase homolytic C–Cl BDEs. W1w theory represents a layered extrapolations to the all-electron CCSD(T)/CBS energy (complete basis-set limit coupled cluster with singles, doubles, and quasiperturbative triple excitations) and achieves an accuracy in the sub-kcal mol^{-1} range for molecules whose wave functions are dominated by dynamical correlation (See Ref. 22 for an overview of the accuracy and applicability of W1w theory and related composite ab initio methods). The methods chosen include conventional DFT, double-hybrid DFT (DHDFT) and a number of composite thermochemical protocols. The conventional DFT exchange-correlation functionals considered in this study (ordered by their rung on Jacob's Ladder)[35] are the pure generalized gradient approximation (GGA) functionals: BLYP,[36,37] B97-D,[38] HCTH407,[39] PBE,[40] BP86,[37,41] and N12;[42] the meta-GGAs (MGGAs): M06-L,[43] TPSS,[44] τ-HCTH,[45] VSXC,[46] M11-L,[47] and MN12-L;[48] the hybrid-GGAs (HGGAs): BH&HLYP,[49] B3LYP,[36,50,51] B3P86,[41,51] B3PW91,[51,52] PBE0,[53] B97-1,[54] B98,[55] X3LYP,[56] and SOGGA-11X;[57] the hybrid-meta-GGAs (HMGGAs): M06,[58] M06-2X,[58] M06-HF,[58] BMK,[59] B1B95,[37,60] TPSSh,[61] and τ-HCTHh;[45] the range-separated (RS) functionals: CAM-B3LYP,[62] LC-ωPBE,[63] ωB97,[64] ωB97X,[64] ωB97X-D,[65] HSE06,[66] HISS,[67] N12-SX,[68] MN12-SX[68] and M11.[69] For selected functionals, we have also included empirical D3 dispersion corrections,[70,71,72] which make use of the Becke–Johnson[73] damping potential as recommended in Ref. 70 (denoted by the suffix -D3). In addition to the conventional DFT procedures, we have also considered the performance of a number of more computationally expensive double-hybrid (DHDFT) procedures (which have been evaluated using both the frozen-core approximation), namely: B2-PLYP,[74] B2GP-PLYP,[75] B2K-PLYP,[76]

ROB2-PLYP,[77] DSD-PBEP86[78] and PWPB95.[79] The conventional DFT methods calculations have been performed in conjunction with the A'VTZ basis set, whilst for the DHDFT procedures, which are known to exhibit slower basis set convergence, the A'VQZ basis set has been employed (with A'VnZ denoting the use of cc-pVnZ for H, the aug-cc-pVnZ basis sets on first-row elements, and the aug-cc-pV(n+d)Z basis sets on second-row elements.[80,81,82] In addition, a number of Gaussian-n thermochemical protocols have been assessed, including: G3X(MP2),[83] G3X(MP2)-RAD,[84] G3X,[83] G3X-RAD,[84] G3-RAD,[84] G4(MP2),[85] G4(MP2)-5H,[86] G4(MP2)-6X,[87] G4,[88] and G4-5H.[86] The performance of the ROCBS-QB3 procedure[89] has also been evaluated. For the benchmarking calculations, the Gaussian-n calculations have been performed on the B3LYP/A'VTZ geometries provided in the Supporting Information of Ref. 33 rather than the prescribed geometries for each method. For the chlorinated derivatives of the nucleobases, pyrimidine and purine derivatives, the geometries of these species have been obtained at the B3LYP/6-31G(2df,p) level, and their validity as equilibrium structures has been confirmed through harmonic vibrational frequency calculations, ensuring that all structures are consist of only real frequencies. To correct the BDEs to 298 K, scaled zero-point vibrational energies (ZPVEs) and thermal corrections for enthalpy (H_{vib}) have been included, using scaling factors taken from the literature, namely 0.9861 for the ZPVE and 0.9909 for the H_{vib} correction.[90] In addition, a spin-orbit coupling correction of 3.52 kJ mol^{-1} has been added to chlorine atom[91] for the G3X(MP2)-RAD calculations involving the chlorinated derivatives of the nucleobases, purine and pyrimidines. All calculations were performed using Gaussian 09 (Revision D.01).[92]

3. Results and Discussion

3.1 Assessment of Theoretical Procedures for the Calculation of Homolytic C–Cl BDEs.

Prior to reporting the homolytic C–Cl BDEs of the chlorinated derivatives of the DNA/RNA nucleobases, and the chlorinated pyrimidine and purines, it is first necessary to identify suitable lower-cost, yet accurate, theoretical procedures that may be used to reliably compute homolytic C–Cl BDEs. A large number of conventional and double-hybrid DFT, as well as a number of composite thermochemical protocols have been assessed for this task. To evaluate these methods, the recently reported CCl28 data set, which consists of 28 homolytic C–Cl BDEs for a diverse range of species containing sp-, sp^2- and sp^3-hybridized C–Cl bonds, obtained by means of the W1w thermochemical protocol. For the purposes of this investigation,

the reference values used to evaluate the various theoretical methods correspond to all-electron, non-relativistic, bottom-of-the-well homolytic C–Cl BDEs, and for the sake of keeping this article self-contained, these reference values are provided in Table 1.

Table 1

All-electron, non-relativistic, bottom-of-the-well homolytic C–Cl BDEs used for evaluating the theoretical methods (kJ mol^{-1})

Molecule	BDE	Molecule	BDE
CH_3Cl (**1**)	369.6	$Cl(H)C=NH$ (**15**)	375.7
$ClC≡CH$ (**2**)	471.8	$ClC≡CCH_3$ (**16**)	476.5
$ClCH_2CHO$ (**3**)	327.3	$H_2C=CHCH_2Cl$ (**17**)	306.2
$ClCH_2CH_2SiH_3$ (**4**)	362.3	CH_2Cl_2 (**18**)	346.0
$ClCH_2CN$ (**5**)	314.0	CH_2FCl (**19**)	371.1
$ClCH_2NH_2$ (**6**)	357.2	$ClC(=O)OH$ (**20**)	371.1
$ClCH_2OH$ (**7**)	363.3	$ClC(=O)NH_2$ (**21**)	364.2
$ClCH_2PH_2$ (**8**)	345.3	$Cl(F)C=CH_2$ (**22**)	411.0
$ClCH_2P(=O)H_2$ (**9**)	358.8	CH_3CH_2Cl (**23**)	372.1
$ClCH_2SH$ (**10**)	333.5	$CH_3C(=O)Cl$ (**24**)	363.5
$ClCH_2SiH_3$ (**11**)	350.1	$ClC(=O)F$ (**25**)	366.9
$ClCH_2S(=O)H$ (**12**)	355.9	$HC(=O)Cl$ (**26**)	362.4
$Cl(H)C=CH_2$ (**13**)	412.4	$CH_3CHClCH_3$ (**27**)	372.8
$Cl(H)C=C=O$ (**14**)	344.3	$CH_3(Cl)C=CH_2$ (**28**)	408.3

Attention is initially given to considering the performance of the conventional and double-hybrid DFT procedures (Table 2). For the conventional DFTs, the A'VTZ basis set has been employed, whilst for the double-hybrid DFTs, the larger A'VQZ basis set has been employed, as it has been shown previously that the DHDFT procedures exhibit slower basis set convergence than conventional DFTs.[93,94] To facilitate a statistical analysis of the performance of these methods, mean absolute deviations (MADs), mean signed deviations (MSDs), largest deviations (LDs, for which the system associated with the largest deviation is indicated in parentheses) and the number of outliers (defined arbitrarily as the number of species with deviations greater than 10 kJ mol^{-1}) are reported.

Table 2

Performance of conventional and double-hybrid DFT methods for the calculation of homolytic C–Cl BDEs (kJ mol^{-1})

Class[a]	Method	MAD[b]	MSD[b]	LD[b]	NO[b]
GGA	BLYP	30.9	–30.9	41.9 (**27**)	27
	B97D	29.1	–29.1	40.3 (**5**)	27
	HCTH407	20.0	–20.0	36.5 (**27**)	26
	BLYP-D3	19.7	–19.7	28.2 (**5**)	27
	N12	14.5	+14.5	37.1 (**2**)	21
	BP86	7.9	–6.2	18.5 (**27**)	9
	PBE-D3	7.1	+6.7	27.2 (**2**)	7
	PBE	5.2	+1.7	23.9 (**2**)	3
	BP86-D3	4.4	+2.4	21.7 (**2**)	3
MGGA	VSXC	25.7	–25.7	43.7 (**5**)	27
	τ-HCTH	19.0	–18.8	35.6 (**27**)	24
	TPSS	17.9	–17.9	28.2 (**27**)	26
	TPSS-D3	11.7	–11.3	19.9 (**5**)	19
	M06-L	7.4	–3.3	16.1 (**27**)	6
	M11-L	7.1	+1.5	14.3 (**26**)	9
	MN12-L	6.4	+1.1	13.6 (**26**)	6
HGGA	BH&HLYP	43.1	–43.1	50.8 (**3**)	28
	B3LYP	28.6	–28.6	38.4 (**27**)	27
	X3LYP	26.5	–26.5	35.7 (**27**)	27
	B3LYP-D3	19.4	–19.4	26.9 (**5**)	27
	B3PW91	16.5	–16.3	28.5 (**27**)	24
	B98	12.8	–12.4	20.8 (**27**)	23
	PBE0	9.5	–8.4	19.2 (**27**)	12
	B3PW91-D3	7.9	–7.1	15.1 (**27**)	8
	B97-1	7.5	–6.5	14.6 (**27**)	6
	B3P86	7.5	–5.7	16.8 (**27**)	8
	SOGGA-11X	6.3	–5.0	16.9 (**2**)	5
	PBE0-D3	5.8	–3.9	12.6 (**27**)	3
HMGGA	TPSSh	20.4	–20.4	30.4 (**27**)	27
	τHCTHh	11.2	–6.9	59.6 (**2**)	12
	M06-HF	9.1	+8.2	19.3 (**14**)	13
	BMK-D3	7.3	+7.3	14.2 (**2**)	5
	M06	5.5	–2.1	12.6 (**28**)	3
	BMK	2.5	+0.4	9.3 (**2**)	0
	M06-2X	1.9	–0.6	6.0 (**28**)	0

RS	CAM-B3LYP	23.7	–23.7	31.3 (**27**)	27
	CAM-B3LYP-D3	19.5	–19.5	25.2 (**27**)	26
	LC-ωPBE	19.3	–19.1	28.5 (**27**)	26
	HISS	17.3	–17.1	27.3 (**27**)	24
	LC-ωPBE-D3	14.6	–14.1	21.2 (**27**)	25
	HSE06	11.5	–10.8	21.7 (**27**)	18
	ωB97XD	8.8	–8.4	14.4 (**27**)	8
	ωB97X	8.3	–7.8	13.8 (**27**)	7
	ωB97	8.1	–7.3	12.2 (**27**)	6
	M11	6.7	–5.8	12.8 (**28**)	4
	N12-SX	6.3	+4.9	25.0 (**2**)	4
	MN12-SX	3.8	+0.2	11.7 (**2**)	1
DHDFT	B2-PLYP	14.2	–13.7	19.3 (**27**)	26
	B2GP-PLYP	10.9	–9.6	14.4 (**16**)	22
	B2-PLYP-D3	10.2	–9.3	13.0 (**16**)	17
	B2K-PLYP	8.8	–6.9	17.1 (**16**)	6
	ROB2-PLYP	8.3	–6.4	18.6 (**16**)	2
	B2GP-PLYP-D3	7.5	–5.8	15.4 (**16**)	1
	B2K-PLYP-D3	7.1	–5.0	18.6 (**16**)	2
	PWPB95	4.5	–2.9	11.0 (**2**)	2
	DSD-PBEP86	4.4	–0.4	22.2 (**16**)	2
	DSD-PBEP86-D3	3.7	+3.1	24.7 (**16**)	2
	PWPB95-D3	2.6	–0.6	12.6 (**2**)	2

[a]GGA = generalized gradient approximation, MGGA = meta-GGA, HGGA = hybrid-GGA, HMGGA = hybrid-meta-GGA, RS = range separated, DHDFT = double-hybrid DFT. [b]MAD = mean absolute deviation, MSD = mean signed deviation, LD = largest deviation (with the system associated with the largest deviation indicated in parentheses), NO = number of outliers (species with deviations greater than 10 kJ mol^{-1}).

From this analysis, a number of key points emerge. Of all of the conventional and double-hybrid DFT methods investigated, only five offer performance below the threshold of chemical accuracy (arbitrarily defined as performance ≤ 4.2 kJ mol^{-1}). The best performing method is M06-2X, with an MAD of just 1.9 kJ mol^{-1}, and an LD of 6.0 kJ mol^{-1}. The BMK procedure also offers reliable performance, with a MAD of 2.5 kJ mol^{-1}. By way of contrast, the worst performance is obtained in the case of BH&HLYP (MAD = 43.1 kJ mol^{-1}). The notably poor performance of BH&HLYP for the computation of BDEs have been reported previously, for example, in the case of N–X (X = H, Cl and Br) bonds.[95,96] The double-hybrid DFT methods offer MADs ranging from 2.6 (PWPB95-D3) to 14.2 (B2-PLYP) kJ mol^{-1}. Second, inclusion of a

D3 dispersion correction is shown, in all but two cases, to improve the performance of the DFT and double-hybrid DFT methods. The performance enhancements typically range from 0.7 kJ mol^{-1} (DSD-PBEP86) to 4.2 (CAM-B3LYP) kJ mol^{-1}. However, especially large improvements are noted in the case of BLYP (11.2), B3LYP (9.2) and B3PW91 (8.6 kJ mol^{-1}). The two functionals which are adversely affected upon inclusion of the D3 correction are PBE and BMK, where deteriorations of 1.9 and 4.8 kJ mol^{-1}, respectively, are noted.

Of the nine GGA functionals investigated, none of these methods offer performance below the threshold of chemical accuracy (i.e., ≤ 4.2 kJ mol^{-1}). The BP86-D3 method offers the best performance of this family of functionals (MAD = 4.4 and LD = 21.7 kJ mol^{-1}), and exhibits a tendency to overestimate the BDEs (MSD = +2.4 kJ mol^{-1}). By way of contrast, the worst performing GGA is BLYP, which has an MAD of 30.9 kJ mol^{-1}, and uniformly underestimates the BDEs (MSD = –30.9 kJ mol^{-1}). Moving now to the MGGA procedures, for which seven such methods have been evaluated, the performance ranges from 6.4 (MN12-L) to 25.7 (VSXC) kJ mol^{-1}. These methods have a general tendency to underestimate the BDEs, with five of the seven methods having MSDs that are negative.

Of the 12 HGGA procedures considered, it can be seen that all tend to underestimate the BDEs. The best performing method is PBE0-D3 (MAD = 5.8 and LD = 12.6 kJ mol^{-1}), with only three species being associated with deviations greater than 10.0 kJ mol^{-1}. The worst performing method is BH&HLYP (MAD = 43.1 and LD = 50.8 kJ mol^{-1}). The popular B3LYP procedure offers relatively poor performance (MAD = 28.6 kJ mol^{-1}), and whilst inclusion of a D3 correction results in a significant improvement, the B3LYP-D3 procedure still offers comparatively poor performance (MAD = 19.4 and LD = 26.9 kJ mol^{-1}). The hybrid-meta GGA procedures feature the two best performing methods of all of the functionals considered, namely M06-2X and BMK, which are associated with MADs of 1.9 and 2.5 kJ mol^{-1}, respectively. Both of these methods have near zero MSDs, and although M06-2X has a slight tendency to underestimate the BDEs (MSD = –0.6 kJ mol^{-1}), BMK has a slight tendency to overestimate them (MSD = +0.4 kJ mol^{-1}). Both methods have relatively low LDs, amounting to 6.0 kJ mol^{-1} in the case of M06-2X and 9.3 kJ mol^{-1} in the case of BMK. The worst performing HMGGA procedure is TPSSh, with an MAD of 20.4 and an LD of 30.4 kJ mol^{-1}.

Turning our attention to the range-separated (RS) procedures, for which twelve such methods have been considered, only one of these methods offers performance below the

threshold of chemical accuracy. In this regard, MN12-SX offers by far the best performance (MAD = 3.8 and LD = 11.7 kJ mol^{-1}), and a near zero MSD (+0.2 kJ mol^{-1}). The next best performing methods are N12-SX and M11, which have MADs of 6.3 and 6.7 kJ mol^{-1}, respectively. The ωB97 family of functionals of Chai and Head-Gordon (*i.e.*, ωB97, ωB97X and ωB97X-D) all offer similar performance, with MADs that range from 8.1 (ωB97) to 8.8 (ωB97XD) kJ mol^{-1}. The worst performing RS procedure is CAM-B3LYP (MAD = 23.7 and LD = 31.3 kJ mol^{-1}), and inclusion of the D3 correction only serves to improve the performance of this method by 4.2 kJ mol^{-1}.

Of the DHDFT procedures, the best performance is noted in the case of PWPB95-D3 (MAD = 2.6 and LD = 12.6 kJ mol^{-1}), whilst the worst performance is exhibited by B2-PLYP (MAD = 14.2 and LD = 19.3 kJ mol^{-1}). The ROB2-PLYP procedure, which compared with B2-PLYP, makes use of a restricted open-shell wave function for radical species offers a significant improvement in performance, with an MAD of 8.3 kJ mol^{-1} (i.e., 5.9 kJ mol^{-1} lower than that for B2-PLYP), although the LD is not greatly affected (being reduced by only 0.7 kJ mol^{-1}). For all of the DHDFTs, inclusion of the D3 correction is advantageous, improving the MADs by amounts ranging from 0.7 (DSD-PBEP86) to 4.0 (B2-PLYP) kJ mol^{-1}.

Attention is now given to evaluating the performance of a number of composite thermochemical protocols. These methods belong to the Gaussian-*n* thermochemical protocols, with the exception of one, namely the restricted-open-shell CBS-QB3 (ROCBS-QB3) procedure. The results of this analysis are provided in Table 3.

Table 3

Performance of various composite thermochemical protocols for the calculation of homolytic C–Cl bond dissociation energies (kJ mol^{-1})

Method	MAD^a	MD^a	LD^a	NO^a
G4	3.9	–3.9	5.5 (**28**)	0
G4(MP2)-6X	3.0	–3.0	6.6 (**16**)	0
G4-5H	2.6	–2.6	5.0 (**1**)	0
G4(MP2)	2.3	–2.1	6.3 (**16**)	0
ROCBS-QB3	2.0	+1.9	4.7 (**12**)	0
G4(MP2)-5H	1.5	–0.8	4.9 (**16**)	0
G3(MP2)-RAD	1.4	–0.6	5.6 (**16**)	0
G3X-RAD	1.4	–1.0	5.2 (**1**)	0
G3X(MP2)-RAD	1.3	–0.4	5.0 (**16**)	0
G3-RAD	1.3	–0.8	4.9 (**1**)	0

^{a}Footnote b of Table 2 applies here.

Of the composite methods that have been investigated, all of the methods offer MADs that are below the threshold of chemical accuracy (i.e., ≤ 4.2 kJ mol^{-1}). Furthermore, none of the composite methods investigated are associated with deviations greater than or equal to 10 kJ mol^{-1}, with G4(MP2)-6X having the largest deviation, amounting to a mere 6.6 kJ mol^{-1}. The cost effective G3X(MP2)-RAD and G3(MP2)-RAD procedures offer impressive performance, with MADs of 1.3 and 1.4 kJ mol^{-1}, respectively, which offer performance that is effectively the same as that of the more computationally expensive G3-RAD and G3X-RAD procedures (which have MADs of 1.3 and 1.4 kJ mol^{-1}, respectively). It is worth pointing out that the G3(MP2)-RAD protocol has been employed previously, for example, in computing homolytic C–Cl BDEs of 30 small chlorinated organic molecules.[97] In contrast, of all the composite methods investigated, the G4 protocol offers the worst performance (MAD = 3.9 kJ mol^{-1}).

3.2 Homolytic C–Cl BDEs of the Chlorinated Derivatives of the Nucleobases, Purine and Pyrimidine.

Having established that the G3X(MP2)-RAD thermochemical protocol offers a cost-effective and reliable approach to calculating C–Cl BDEs (with an MAD of 1.3 and an LD of 5.0 kJ mol^{-1}), this method is now applied to computing homolytic C–Cl BDEs for the chlorinated

derivatives of the nucleobases (namely adenine, cytosine, guanine, thymine and uracil), as well as those of purine and pyrimidine (Fig. 1).
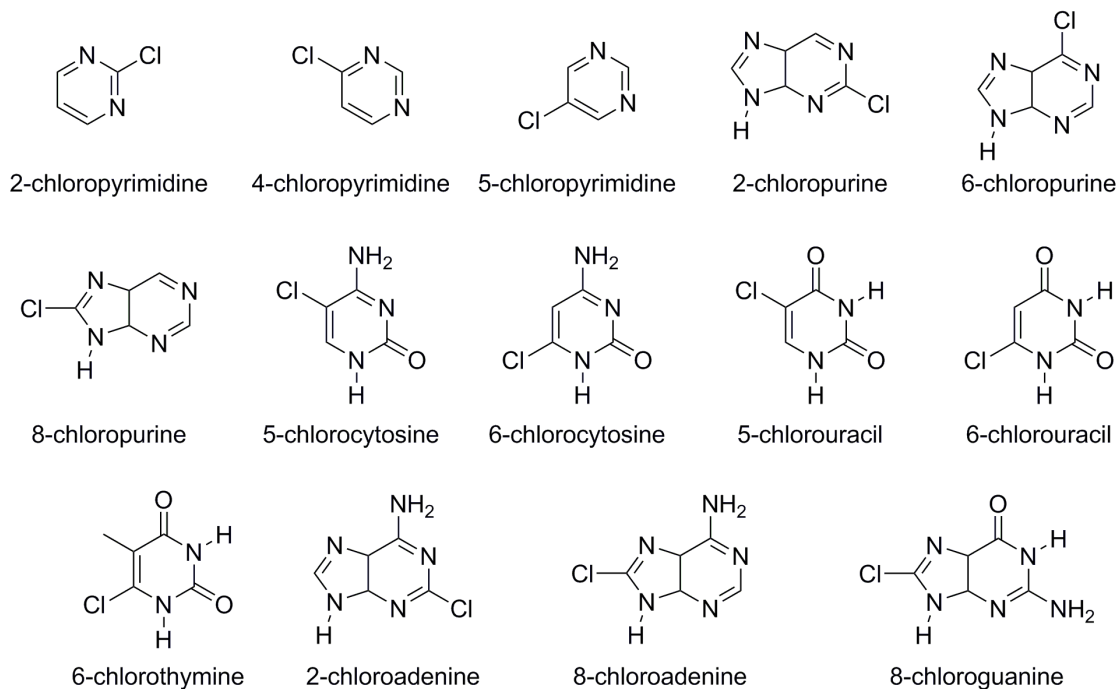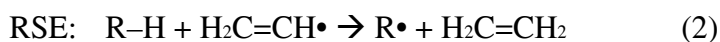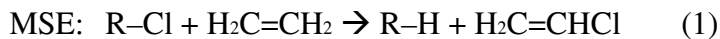

Figure 1. Structures of the chlorinated derivatives of the DNA/RNA nucleobases, as well as those of pyrimidine and purine

The BDEs (at 298 K) for these species are provided in Table 4 (electronic and ZPVE-corrected BDEs are available in Table S2 of the Supporting Information). In addition, we also consider how the substituents govern the BDEs, compared with the BDE of chloroethene, by considering the effect of substituents in both the closed-shell chlorinated reactants, as well as the carbon-centered radical products. To do this, we report molecule stabilization energies (MSEs, Eq. 1), and radical stabilization energies (RSEs, Eq. 2), which represent isodesmic reactions in which transfer of atoms is occurring between sp^2-hybridzed carbon atoms.

$$\text{MSE:} \quad \text{R–Cl} + \text{H}_2\text{C}=\text{CH}_2 \rightarrow \text{R–H} + \text{H}_2\text{C}=\text{CHCl} \qquad (1)$$

$$\text{RSE:} \quad \text{R–H} + \text{H}_2\text{C}=\text{CH}\bullet \rightarrow \text{R}\bullet + \text{H}_2\text{C}=\text{CH}_2 \qquad (2)$$

Defined in this way, a positive value for the MSE indicates a relative stabilizing effect of the chlorinated closed-shell precursor species compared with chloroethene, whilst a negative MSE value indicates relative destabilization. Regarding relative radical stability, a positive RSE value indicates that for a given radical, such a system is destabilized relative to the ethene radical, whilst a negative value indicates relative stabilization of the product radical compared with the prototypical ethene radical. It follows that the sum of the MSE and RSE values for a given system provides the relative BDE of that system compared with the BDE of chloroethene.

Table 4

Gas-Phase Homolytic C–Cl bond dissociation energies for the chlorinated derivatives of nucleobases, purine and pyrimidine (See Figure 1 for structures), as well as molecule stabilization energies (MSEs) and radical stabilization energies (RSEs) (298 K, kJ mol^{-1}, and bond lengths in Å)

Molecule	BDE$_{298}$	MSE	RSE	$r_{C–Cl}$
4-chloropyrimidine	391.0	+6.8	–12.1	1.749
6-chloropurine	393.2	+5.3	–8.4	1.740
2-chloropyrimidine	395.8	+2.7	–3.2	1.748
chloroethene	396.3	0.0	0.0	1.745
2-chloropurine	397.6	+0.9	+0.4	1.748
2-chloroadenine	397.8	+4.0	–2.5	1.755
6-chlorocytosine	403.6	–3.0	+10.3	1.736
6-chlorouracil	404.8	–7.0	+15.5	1.733
6-chlorothymine	406.7	–5.9	+16.2	1.739
5-chloropyrimidine	409.1	–4.6	+17.4	1.740
5-chlorocytosine	416.0	–8.4	+28.1	1.747
5-chlorouracil	417.2	–18.7	+39.6	1.728
8-chloropurine	417.8	–5.7	+27.1	1.715
8-chloroadenine	418.8	–5.7	+28.2	1.718
8-chloroguanine	419.1	–6.5	+29.2	1.719

On the basis of the data presented in Table 4, a number of general points emerge. First, for all of the species investigated, 4-chloropyrimidine has the lowest BDE (391.0 kJ mol^{-1}) whilst 8-chloroguanine has the largest (419.1 kJ mol^{-1}). These BDEs may be compared with the BDE of chloroethene, which is computed to be 396.3 kJ mol^{-1}. Second, concerning the C–Cl

bond lengths, the 8-chloro derivatives of purine, adenine and guanine have the shortest C–Cl distances (1.715–1.719 Å), whilst the longest distance is observed in the case of 2-chloroadenine (1.755 Å), which is 0.01 Å longer than that of chloroethene (1.745 Å). Third, concerning the MSE and RSE values for each system, in all but one case (2-chloropurine), the two values adopt opposite signs. This indicates that, for example, both the closed-shell chlorinated parent and the product radicals are either relatively stabilized, or that they are both relatively destabilized (compared with chloroethene or the ethene radical). Regarding the MSEs (which effectively compare the relative stability of a given chlorinated molecule compared with chloroethene), the most relatively stabilized chlorinated species are 4-chloropyrimidine and 6-chloropurine (MSEs = +6.8 and +5.3 kJ mol^{-1}, respectively), whilst 5-chlorouracil is by far the most destabilized chlorinated molecule (MSE = –18.7 kJ mol^{-1}), followed by 5-chlorocytosine (MSE = –8.4 kJ mol^{-1}). Finally, concerning the RSEs (which effectively compare the relative stability of a given radical with that of the ethene radical), the most stabilized radical appears to be that derived from 4-chloropyrimidine (RSE = –12.1 kJ mol^{-1}), followed by that derived from 6-chloropurine (RSE = –8.4 kJ mol^{-1}). The most destabilized radical corresponds to that derived from 5-chlorouracil (RSE = +39.6 kJ mol^{-1}), presumably because of the strong inductive effect of the adjacent carbonyl group.

Attention is now turned to considering the BDEs of the isomeric species of the pyrimidine and purine derivatives. Beginning with the BDEs of the pyrimidine derivatives, the BDEs of these species increase in the order: 4-chloropyrimidine (391.0 kJ mol^{-1}) < 2-chloropyrimidine (395.8 kJ mol^{-1}) < 5-chloropyrimidine (409.1 kJ mol^{-1}). Although 4-chloropyrimidine is associated with the largest relative stabilizing effect (MSE = +6.8 kJ mol^{-1}) of any of the chloropyrimidine derivatives (with the other two species having MSE values of +2.7 and –4.6 kJ mol^{-1}), it has the lowest BDE. This lower BDE arises because of the especially large relative stabilizing effect in the product radical (RSE = –12.1 kJ mol^{-1}), which is of significantly greater magnitude than the relative stabilizing effect present in the chlorinated precursor. In contrast, the much larger BDE of 5-chloropyrimidine (409.1 kJ mol^{-1}) arises because of the existence of a significant destabilizing effect in the product radical (RSE = +17.4 kJ mol^{-1}), which is of much larger magnitude than the destabilizing effect present in the chlorinated parent (MSE = –4.6 kJ mol^{-1}). Turning our attention to the purine derivatives, the BDEs increase in the order: 6-chloropurine (393.2 kJ mol^{-1}) < 2-chloropurine (397.6 kJ mol^{-1}) <

8-chloropurine (417.8 kJ mol^{-1}). Of the three isomeric closed-shell chlorinated precursors, the 6-chloro isomer has the lowest energy (MSE = +5.3 kJ mol^{-1}, being relatively stabilized compared with respect to chloroethene), but has the lowest BDE because the product radical is subject to stabilizing interactions of even greater magnitude (RSE = –8.4 kJ mol^{-1}). The larger BDE of 8-chloropurine (417.8 kJ mol^{-1}) arises because of the significantly larger relative destabilizing effect present in the radical (RSE = +27.1 kJ mol^{-1}), which dominates over the much smaller destabilizing effect present in the chlorinated parent (MSE = –5.7 kJ mol^{-1}).

Attention is now turned to considering the BDEs of the isomeric chlorinated derivatives of adenine, cytosine and uracil. Beginning with the chloroadenine derivatives, the BDEs of these two species differ by 21.0 kJ mol^{-1}, with 2-chloroadenine being associated with a BDE of 397.8 kJ mol^{-1}, and 8-chloroadenine with a BDE of 418.8 kJ mol^{-1}. Although 8-chloroadenine lies 9.7 kJ mol^{-1} higher in energy than 2-chloroadenine, the product radical arising via dissociation of 8-chloroadenine lies 30.7 kJ mol^{-1} higher in energy than the radical arising via dissociation of the 2-chloro isomer. Consequently, the significantly larger BDE of the 8-chloro versus the 2-chloro isomer arises because of especially large relative destabilizing effects in the product radical. Turning our attention to the 5- and 6-chloro isomers of cytosine, the 5-chloro isomer has the largest BDE (416.0 vs 403.6 kJ mol^{-1}). Although the 5-chloro isomer is lies 5.4 kJ mol^{-1} higher in energy than the 6-chloro isomer (with both species being destabilized relative to chloroethene, with MSEs of –8.4 and –3.0 kJ mol^{-1}, respectively), the radical derived from 5-chlorocytosine lies 17.8 kJ mol^{-1} higher in energy than that derived from the 6-chloro isomer, and thus it is the greater relative instability of the product radical that gives rise to the larger BDE in the case of 5-chlorocytosine. Finally, concerning the uracil derivatives, the 5-chloro isomer has a BDE (417.2 kJ mol^{-1}) that is 12.4 kJ mol^{-1} higher than that of 6-chlorouracil. Although 5-chlorouracil lies 11.7 kJ mol^{-1} higher in energy than 6-chlorouracil (and with both species being destabilized relative to chloroethene, with MSEs of –18.7 and –7.0 kJ mol^{-1}, respectively), the larger BDE of the former again arises because of a greater magnitude of destabilizing effects in the product radical (with the radical derived from 5-chlorouracil lying 24.1 kJ mol^{-1} higher in energy than that derived from 6-chlorouracil).

It is insightful to compare the C–Cl BDEs for a subset of the chlorinated species considered in this study, with the C–Br BDEs of the corresponding brominated species for which data has recently been reported (at the G4 level).[98] Beginning with the halogenated ethene

derivatives, the C–Cl BDE of chloroethene (396.3 kJ mol⁻¹) is 63.7 kJ mol⁻¹ higher than the C–Br BDE of bromoethene. Concerning the brominated nucleobases, compared with the C–Br BDEs of the four brominated nucleobase derivatives considered in that study (namely 8-bromoguanine (345.3), 8-bromoadenine (345.6), 5-bromocytosine (348.8) and 5-bromouracil (350.3 kJ mol⁻¹)), the C–Cl BDEs are higher by between 66.9–73.8 kJ mol⁻¹.

Finally, we note that the M06-2X and MN12-SX DFT procedures (which represent the best performing HMGGA and RS functionals, respectively) afford C–Cl BDEs that are in good qualitative agreement with those obtained using the more computationally-expensive G3X(MP2)-RAD procedure (the results of these investigations are provided in Table S3 of the Supporting Information). When compared with the G3X(MP2)-RAD results, the largest deviations for both functionals are observed in the case of 6-chlorothymine. In this regard, M06-2X gives a deviation of 6.2 kJ mol⁻¹, whilst MN12-2X is in much better agreement, with a deviation of just 3.1 kJ mol⁻¹.

Conclusions

The chlorinated derivatives of nucleobases (and nucleosides), as well as those of purine, have well-established anticancer activity, and in some cases, are also shown to be involved in the link between chronic inflammatory conditions and the development of cancer. In this study, the stability of such species toward radical formation arising by way of homolytic C–Cl bond cleavage has been studied. Initially, the performance of a wide range of contemporary theoretical procedures have been assessed for their ability to accurately compute C–Cl BDEs, relative to a recently reported set of 28 C–Cl BDEs (known as the CCl28 dataset) obtained using the benchmark-quality W1w thermochemical protocol. Of the conventional DFT methods, M06-2X in conjunction with the aug'-cc-pV(T+d)Z basis set offers the most reliable performance (MAD = 1.9 kJ mol⁻¹), whilst the BMK functional also offers good performance (MAD = 2.5 kJ mol⁻¹). Of the double-hybrid DFT methods (evaluated in conjunction with the aug'-cc-pV(Q+d)Z basis set), PWPB95-D3 offers the best performance (MAD = 2.6 kJ mol⁻¹), followed by DSD-PBEP86-D3 (MAD = 3.7 kJ mol⁻¹). Of the ten composite thermochemical protocols evaluated, all achieve MADs less than 4.2 kJ mol⁻¹, with G3-RAD and G3X(MP2)-RAD offering the lowest MADs (1.3 kJ mol⁻¹). Using the G3X(MP2)-RAD procedure, the BDEs of the chlorinated isomers of adenine, cytosine, guanine, thymine, uracil, purine and pyrimidine have been

computed. Of these species, 4-chloropyrimidine has the lowest BDE (391.0 kJ mol^{-1}) whilst 8-chloroguanine has the largest (419.1 kJ mol^{-1}).

Supporting Information

This article contains the following Supporting Information: Geometries of the chlorinated derivatives of the DNA/RNA nucleobases, purine and pyrimidine (obtained at the B3LYP/6-31G(2df,p) level) (Table S1), and electronic and ZPVE-inclusive G3X(MP2)-RAD homolytic C–Cl BDEs, MSEs and RSEs for the chlorinated derivatives of the nucleobases, purine and pyrimidine (Table S2), and homolytic C–Cl BDEs (298 K) for the chlorinated nucleobase, purine and pyrimidine derivatives obtained using two well-performing conventional DFTs (M06-2X and MN12-SX) in conjunction with the A'VTZ basis set (Table S3).

References

[1] G. R. Goodman, C. Burian, J. A. Koziol, A. Saven, *J. Clin. Oncol.* **2003**, *21*, 891.
[2] L. D. Piro, C. J. Carrera, D. A. Carson, E. Beutler, *N. Engl. J. Med.* **1990**, *322*, 1117.
[3] T. P. Leist, R. Weissert, *Clin. Neuropharmacol.* **2011**, *34*, 28.
[4] T. P. Leist, P. Vermersch, *Curr. Med. Res. Opin.* **2007**, *23*, 2667.
[5] F. Bontemps, A. Delacauw, S. Cardoen, E. Van Den Neste, G. Van Den Berghe, *Biochem. Pharmacol.* **2000**, *59*, 1237.
[6] S. Lindemalm, J. Liliemark, G. Juliusson, R. Larsson, F. Albertioni, *Cancer Lett.* **2004**, *210*, 171.
[7] A. Bendich, P. J. Russell Jr, J. J. Fox, *J. Am. Chem. Soc.* **1954**, *76*, 6073.
[8] A. C. Sartorelli, B. A. Booth, *Cancer Res.* **1960**, *20*, 198.
[9] E. Magdon, *Naturwissenschaften* **1966**, *53*, 44.
[10] B. I. Fedeles, B. D. Freudenthal, E. Yau, V. Singh, S. C. Chang, D. Li, J. C. Delaney, S. H. Wilson, J. M. Essigmann, *Proc. Natl. Acad. Sci. USA.* **2015**, *112*, E4571.
[11] V. V. Lao, J. L. Herring, C. H. Kim, A. Darwanto, U. Soto, L. C. Sowers, *Carcinogenesis* **2009**, *30*, 886.

[12] A. Patra, J. Harp, P. S. Pallan, L. Zhao, M. Abramov, P. Herdewijn, M. Egli, *Nucl. Acids Res.* **2013**, *41*, 2689.

[13] S. M. Morris, *Mutat. Res.* **1993**, *297*, 39.

[14] M. Masuda, T. Suzuki, M. D. Friesen, J. L. Ravanat, J. Cadet, B. Pignatelli, H. Nishino, H. Ohshima, *J. Biol. Chem.* **2001**, *276*, 40486.

[15] V. K. Rastogi, M. A. Palafox, K. Lang, S. K. Singhal, R. K. Soni, R. Sharma, *Indian J. Pure Appl. Phys.* **2006**, *44*, 653.

[16] M. A. Palafox, V. K. Rastogi, *Asian Chem. Lett.* **2015**, *19*, 1.

[17] S. Ortiz, M. C. Alvarez-Ros, M. A. Palafox, V. K. Rastogi, V. Balachandran, S. K. Rathor, *Spectrochim. Acta A Mol. Biomol. Spectrosc.* **2014**, *130*, 653.

[18] M. J. Nowak, H. Rostkowska, L. Lapinski, J. S. Kwiatkowski, J. Leszczynski, *J. Phys. Chem.* **1994**, *98*, 2813.

[19] Y. Xue, D. Xu, D. Xie, G. Yan, *Spectrochim. Acta A Mol. Biomol. Spectrosc.* **2000**, *56A*, 1929.

[20] S. D. Wetmore, R. J. Boyd, L. A Eriksson, *Chem. Phys. Lett.* **2001**, *343*, 151.

[21] F. Kossoski, J. Kopyra, M. T. Varella, *Phys. Chem. Chem. Phys.* **2015**, *17*, 28958.

[22] A. Karton, *WIREs Comput. Mol. Sci.* **2016**, *6*, 292.

[23] L. A. Curtiss, P. C. Redfern, K. Raghavachari, *WIREs Comput. Mol. Sci.* **2011**, 1, 810.

[24] K. A. Peterson, D. Feller, D. A. Dixon, *Theor. Chem. Acc.* **2012**, *131*, 1079.

[25] M. L. Stover, V. E. Jackson, M. H. Matus, M. A. Adams, C. J. Cassady, D. A. Dixon, *J. Phys. Chem. B* **2012**, *116*, 2905.

[26] A. Karton, J. M. L. Martin, *J. Chem. Phys.* **2012**, *136*, 124114.

[27] R. O. Ramabhadran, A. Sengupta, K. Raghavachari, *J. Phys. Chem. A* **2013**, *117*, 4973.

[28] O. V. Dorofeeva, O. N. Ryzhova, *J. Phys. Chem. A* **2014**, *118*, 3490.

[29] A. Karton, L.-J. Yu, M. K. Kesharwani, J. M. L. Martin, *Theor. Chem. Acc.* **2014**, *133*, 1483.

[30] M. K. Kesharwani, A. Karton, J. M. L. Martin, *J. Chem. Theory Comput.* **2016**, *12*, 444.

[31] B. Chan, A. Karton, C. J. Easton, L. Radom, *J. Chem. Theory Comput.* **2016**, *12*, 1606.

[32] K. M. Uddin, D. J. Henry, R. A. Poirier, P. L. Warburton, *Theor. Chem. Acc.* **2016**, *135*, 224.

[33] A. Garifullina, A. Mahboob, R. J. O'Reilly, *Chem. Data Collect.* **2016**, *3*, 21.

[34] J. M. L. Martin, G. de Oliveira, *J. Chem. Phys.* **1999**, *111*, 1843.

[35] J. P. Perdew, K. Schmidt, *AIP Conf. Proc.* **2001**, *577*, 1.

[36] C. Lee, W. Yang, R. G. Parr, *Phys. Rev. B* **1988**, *37*, 785.

[37] A. D. Becke, *Phys. Rev. A* **1988**, *38*, 3098.

[38] S. Grimme, *J. Comput. Chem.* **2006**, *27*, 1787.

[39] A. D. Boese, N. C. Handy, *J. Chem. Phys.* **2001**, 1*14*, 5497.

[40] J. P. Perdew, K. Burke, M. Ernzerhof, *Phys. Rev. Lett.* **1996**, *77*, 3865; ibid *Phys. Rev. Lett.* **1997**, *78*, 1396.

[41] J. P. Perdew, *Phys. Rev. B* **1986**, *33*, 8822.

[42] R. Peverati, D. G. Truhlar, *J. Chem. Theory Comput.* **2012**, *8*, 2310.

[43] Y. Zhao, D. G. Truhlar, *J. Chem. Phys.* **2006**, *125*, 194101.

[44] J. M. Tao, J. P. Perdew, V. N. Staroverov, G. E. Scuseria, *Phys. Rev. Lett.* **2003**, *91*, 146401.

[45] A. D. Boese, N. C. Handy, *J. Chem. Phys.* **2002**, *116*, 9559.

[46] T. van Voorhis, G. E. Scuseria, *J. Chem. Phys.* **1998**, *109*, 400.

[47] R. Peverati, D. G. Truhlar, *J. Phys. Chem. Lett.* **2012**, *3*, 117.

[48] R. Peverati, D. G. Truhlar, *Phys. Chem. Chem. Phys.* **2012**, *10*, 13171.

[49] A. D. Becke, *J. Chem. Phys.* **1993**, *98*, 1372.

[50] P. J. Stephens, F. J. Devlin, C. F. Chabalowski, M. J. Frisch, *J. Phys. Chem.* **1994**, *98*, 11623.

[51] A. D. Becke, *J. Chem. Phys.* **1993**, *98*, 5648.

[52] J. P. Perdew, J. A. Chevary, S. H. Vosko, K. A. Jackson, M. R. Pederson, D. J. Singh, C. Fiolhais, *Phys. Rev. B* **1992**, *46*, 6671.

[53] C. Adamo, V. Barone, *J. Chem. Phys.* **1999**, *110*, 6158.

[54] F. A. Hamprecht, A. J. Cohen, D. J. Tozer, N. C. Handy, *J. Chem. Phys.* **1998**, *109*, 6264.

[55] H. L. Schmider, A. D. Becke, *J. Chem. Phys.* **1998**, *108*, 9624.

[56] X. Xu, Q. Zhang, R. P. Muller, W. A. Goddard, *J. Chem. Phys.* **2005**, *122*, 014105.

[57] R. Peverati, D. G. Truhlar, *J. Chem. Phys.* **2011**, *135*, 191102.

[58] Y. Zhao, D. G. Truhlar, *Theor. Chem. Acc.* **2008**, *120*, 215.

[59] A. D. Boese, J. M. L. Martin, *J. Chem. Phys.* **2004**, *121*, 3405.

[60] A. D. Becke, *J. Chem. Phys.* **1996**, *104*, 1040.

[61] V. N. Staroverov, G. E. Scuseria, J. Tao, J. P. Perdew, *J. Chem. Phys.* **2003**, *119*, 12129.

[62] T. Yanai, D. Tew, N. Handy, *Chem. Phys. Lett.* **2004**, *393*, 51.

[63] O. A. Vydrov, G. E. Scuseria, *J. Chem. Phys.* **2006**, *125*, 234109.

[64] J.-D. Chai, M. Head-Gordon, *J. Chem. Phys.* **2008**, *128*, 084106.

[65] J.-D. Chai, M. Head-Gordon, *Phys. Chem. Chem. Phys.* **2008**, *10*, 6615.

[66] J. Heyd, G. E. Scuseria, M. Ernzerhof, *J. Chem. Phys.* **2003**, *118*, 8207.

[67] T. M. Henderson, A. F. Izmaylov, G. E. Scuseria, A. Savin, *J. Chem. Theory Comput.* **2008**, *4*, 1254.

[68] R. Peverati, D. G. Truhlar, *Phys. Chem. Chem. Phys.* **2012**, *14*, 16187.

[69] R. Peverati, D. G. Truhlar, *J. Phys. Chem. Lett.* **2011**, *2*, 2810.

[70] S. Grimme, E. Ehrlich, L. Goerigk, *J. Comput. Chem.* **2011**, *32*, 1456.

[71] S. Grimme, J. Antony, S. Ehrlich, H. Krieg, *J. Chem. Phys.* **2010**, *132*, 154104.

[72] S. Grimme, *WIREs Comput. Mol. Sci.* **2011**, *1*, 211.

[73] A. D. Becke, E. R. Johnson, *J. Chem. Phys.* **2005**, *123*, 154101.

[74] S. Grimme, *J. Chem. Phys.* **2006**, *124*, 034108.

[75] A. Karton, A. Tarnopolsky, J.–F. Lamere, G. C. Schatz, J. M. L. Martin, *J. Phys. Chem. A* **2008**, *112*, 12868.

[76] A. Tarnopolsky, A. Karton, R. Sertchook, D. Vuzman, J. M. L. Martin, *J. Phys. Chem. A* **2008**, *112*, 3.

[77] D. C. Graham, A. S. Menon, L. Goerigk, S. Grimme, L. Radom, *J. Phys. Chem. A* **2009**, *113*, 9861.

[78] S. Kozuch, J. M. L. Martin, *Phys. Chem. Chem. Phys.* **2011**, *13*, 20104.

[79] L. Goerigk, S. Grimme, *J. Chem. Theory Comput.* **2011**, *7*, 291.

[80] T. H. Dunning, Jr., *J. Chem. Phys.* **1989**, *90*, 1007.

[81] R. A. Kendall, T. H. Dunning, Jr., R. J. Harrison, *J. Chem. Phys.* **1992**, *96*, 6796.

[82] T. H. Dunning, K. A. Peterson, A. K. Wilson, *J. Chem. Phys.* **2001**, *114*, 9244.

[83] L. A. Curtiss, P. C. Redfern, K. Raghavachari, J. A. Pople, *J. Chem. Phys.* **2001**, *114*, 108.

[84] D. J. Henry, M. B. Sullivan, L. Radom, *J. Chem. Phys.* **2003**, *118*, 4849.

[85] L. A. Curtiss, P. C. Redfern, K. Raghavachari, *J. Chem. Phys.* **2007**, *127*, 124105.

[86] B. Chan, M. L. Coote, L. Radom, *J. Chem. Theory Comput.* **2010**, *6*, 2647.

[87] B. Chan, J. Deng, L. Radom, *J. Chem. Theory Comput.* **2011**, *7*, 112.

[88] L. A. Curtiss, P. C. Redfern, K. Raghavachari, *J. Chem. Phys.* **2007**, *126*, 084108.

[89] G. P. Wood, L. Radom, G. A. Petersson, E. C. Barnes, M. J. Frisch, J. A. Montgomery Jr, *J. Chem. Phys.* **2006**, *125*, 094106(1-16).

[90] J. P. Merrick, D. Moran, L. Radom, *J. Phys. Chem. A* **2007**, *111*, 11683.

[91] L. A. Curtiss, M. P. McGrath, J.-P. Blaudeau, N. E. Davis, R. C. Binning, L. Radom, *J. Chem. Phys.* **1995**, *103*, 6104.

[92] Gaussian 09, Revision D.01, M. J. Frisch, G. W. Trucks, H. B. Schlegel, G. E. Scuseria, M. A. Robb, J. R. Cheeseman, G. Scalmani, V. Barone, B. Mennucci, G. A. Petersson, H. Nakatsuji, M. Caricato, X. Li, H. P. Hratchian, A. F. Izmaylov, J. Bloino, G. Zheng, J. L. Sonnenberg, M. Hada, M. Ehara, K. Toyota, R. Fukuda, J. Hasegawa, M. Ishida, T. Nakajima, Y. Honda, O. Kitao, H. Nakai, T. Vreven, J. A. Montgomery, Jr., J. E. Peralta, F. Ogliaro, M. Bearpark, J. J. Heyd, E. Brothers, K. N. Kudin, V. N. Staroverov, R. Kobayashi, J. Normand, K. Raghavachari, A. Rendell, J. C. Burant, S. S. Iyengar, J. Tomasi, M. Cossi, N. Rega, J. M. Millam, M. Klene, J. E. Knox, J. B. Cross, V. Bakken, C. Adamo, J. Jaramillo, R. Gomperts, R. E. Stratmann, O. Yazyev, A. J. Austin, R. Cammi, C. Pomelli, J. W. Ochterski, R. L. Martin, K. Morokuma, V. G. Zakrzewski, G. A. Voth, P. Salvador, J. J. Dannenberg, S. Dapprich, A. D. Daniels, Ö. Farkas, J. B. Foresman, J. V. Ortiz, J. Cioslowski, and D. J. Fox, Gaussian, Inc., Wallingford CT, 2009.

[93] L. Goerigk, S. Grimme, *WIREs Comput. Mol. Sci.* **2014**, *4*, 576.

[94] A. Karton, J. M. L. Martin, *J. Chem. Phys.* **2011**, *135*, 144119.

[95] R. J. O'Reilly, A. Karton, L. Radom, *Int. J. Quantum Chem.* **2012**, *112*, 1862.

[96] R. J. O'Reilly, A. Karton, *Int J Quantum Chem.* **2016**, *116*, 52.

[97] M. L. Coote, C. Y. Lin, A. A. Zavitsas, *Phys. Chem. Chem. Phys.* **2014**, *16*, 8686.

[98] Z. Kazakbayeva, S. Zhumagali, A. Mahboob, R. J. O'Reilly, *Chem. Data Collect.* **2016**, *2*, 43.